# Measurement of the Rate Distribution of the Population of Repeating Fast Radio Bursts: Implications for Progenitor Models

C. W. James[1] , S. Osłowski[2] , C. Flynn[2] , P. Kumar[2] , K. Bannister[3] , S. Bhandari[3] , W. Farah[2] , M. Kerr[4] ,
D. R. Lorimer[5,6] , J.-P. Macquart[1] , C. Ng[7] , C. Phillips[3], D. C. Price[2,8] , H. Qiu[3,9] , R. M. Shannon[2], and R. Spiewak[10]

[1] International Centre for Radio Astronomy Research, Curtin University, Bentley, WA 6102, Australia; clancy.james@curtin.edu.au
[2] Centre for Astrophysics and Supercomputing, Swinburne University of Technology, Mail H30, P.O. Box 218, VIC 3122, Australia
[3] CSIRO Astronomy & Space Science, Australia Telescope National Facility, P.O. Box 76, Epping, NSW 1710, Australia
[4] Space Science Division, Naval Research Laboratory, Washington, DC 20375, USA
[5] Department of Physics and Astronomy, West Virginia University, P.O. Box 6315, Morgantown, WV 26506, USA
[6] Center for Gravitational Waves and Cosmology, West Virginia University, Chestnut Ridge Research Building, Morgantown, WV 26505, USA
[7] Dunlap Institute for Astronomy and Astrophysics, University of Toronto, 50 St. George Street, Toronto, ON M5S 3H4, Canada
[8] Department of Astronomy, University of California Berkeley, Berkeley, CA 94720, USA
[9] Sydney Institute for Astronomy, School of Physics, University of Sydney, Sydney, NSW 2006, Australia
[10] ARC Centre of Excellence for Gravitational Wave Discovery (OzGrav), Australia
Received 2019 December 17; revised 2020 March 22; accepted 2020 May 1; published 2020 May 22

## Abstract

The discovery of many repeating fast radio bursts (FRBs) by the Canadian Hydrogen Intensity Mapping Experiment, the high rate of individual bursts, and the observation of repeat bursts from a bright FRB initially detected by the Australian Square Kilometre Array Pathfinder (ASKAP) suggest a significant population of repeating FRBs. Here, we analyze the rate distribution of this population using results from follow-up observations of the Commensal Real-time ASKAP Fast Transients Survey. Characterizing a repeating FRB by its burst rate $R_0$ above an energy of $10^{38}$ erg, we consider a volumetric density $\Phi(R_0)$ with rate distribution $d\Phi \propto R_0^\zeta dR_0$. We use maximum-likelihood methods to constrain $\zeta < -1.94$ at 90% confidence. We discuss how this constraint can be used to limit different classes of progenitor models for repeating FRBs: it excludes FRBs with burst rate proportional to neutron star spin-down power with braking index $n \leqslant 14$, i.e., magnetic dipole radiation ($n = 3$); and it excludes some scenarios for FRB emission from magnetars, and the magnetic field interactions of compact binaries.

*Unified Astronomy Thesaurus concepts:* Radio transient sources (2008); Neutron stars (1108); Magnetars (992); Astrostatistics (1882); Radio bursts (1339); Compact binary stars (283)

## 1. Introduction

The discovery of FRB 121102 (Spitler et al. 2014, 2016) raised the prospect that all fast radio bursts (FRBs) may emit repeat bursts at some level (e.g., Caleb et al. 2018). Of the many classes of models for FRB emission, those leading to long-term repeat emission tend to invoke a young, highly magnetized object—a neutron star (NS) or white dwarf—as the central engine (e.g., Kashiyama et al. 2013; Lyubarsky 2014; Pen & Connor 2015; Zhang & Zhang 2017), while models producing one-off bursts tend to involve the cataclysmic merger of compact objects (e.g., Totani 2013; Zhang 2014; Wang et al. 2016). Both scenarios need to account for the now-confirmed cosmological origin of FRBs (Bannister et al. 2019; Prochaska et al. 2019; Marcote et al. 2020).

Discoveries of repeating FRBs continue. So far, a total of nine from the Canadian Hydrogen Intensity Mapping Experiment (CHIME; CHIME/FRB Collaboration et al. 2019a; The CHIME/FRB Collaboration et al. 2019), one from the bright population of Australian Square Kilometre Array Pathfinder (ASKAP) FRBs (Kumar et al. 2019; Patek & CHIME/FRB Collaboration 2019), and one from the Large Phased Array (Fedorova & Rodin 2019) have been reported. Additionally, Ravi (2019) has calculated that the rate of single bursts observed by CHIME (CHIME/FRB Collaboration et al. 2019b), regardless of origin, is at least $2 \times 10^4$ yr$^{-1}$ Gpc$^{-3}$, well in excess of all proposed populations of cataclysmic events. This argues that even if there exists a subpopulation of

one-off bursts, the majority of all bursts are produced by repeating objects.

Extensive follow-up observations of 27 ASKAP FRBs by the Commensal Real-time ASKAP Fast Transients (CRAFT; Macquart et al. 2010) collaboration have detected repeat emission from only FRB 171019, and have ruled out 19 as repeating as regularly as FRB 121102 (James et al. 2019a). Indeed, James (2019) showed that if all FRBs repeat, then the majority must repeat at much lower rates than FRB 121102.

Combined, this evidence strongly suggests a large population of FRBs that repeat at rates much lower than typical observation times, but which combine to produce the majority of observed bursts. Indeed, whatever mechanism is powering repeating FRBs, it seems unlikely to maintain a high power output over cosmological timescales. This is certainly the case for the aforementioned models invoking a young, magnetized compact object. Clearly, the microphysics of emission will determine the "fine" properties of bursts from any given repeater: the presence or otherwise of subpulses (Hessels et al. 2019), the power-law index of its burst energy distribution (Law et al. 2017), the burst time structure (Ravi et al. 2016; Farah et al. 2018; Oslowski et al. 2018) and distribution (Oppermann et al. 2018), and the burst spectral structure (Macquart et al. 2019). These could feasibly change over the lifetime of a repeating FRB, as evinced by the differences between repeating and as-yet non-repeating populations (The CHIME/FRB Collaboration et al. 2019). However, loss of

energy by a central engine must eventually result in a reduction in the regularity and/or energy of bursts from a repeating FRB.

The population of repeating FRBs could therefore be described as the differential density $d\Phi(R_0)/dR_0$ of repeating FRBs per unit volume, with repetition rates above an energy threshold $E_0$ between $R_0$ and $R_0 + dR_0$. In this Letter we use an NS spin-down model to motivate a power-law form of $d\,\Phi(R_0)$, and derive the power-law index using recent data from CRAFT. We then proceed to show it is consistent with the distribution of repetition rates observed by CHIME, and can be used to limit a number of progenitor models for repeating FRBs.

## 2. Neutron Star Spin-down Model

The standard model for NS spin-down is magnetic dipole radiation (MDR; e.g., Shapiro & Teukolsky 1986). MDR predicts a decrease in an individual pulsar's angular frequency $\omega$ with time according to $\dot{\omega} \propto \omega^n$, where the braking index $n = 3$, and $\dot{x}$ denotes the time derivative of a parameter $x$. This can be compared to spin-down due to the emission of gravitational waves ($n = 5$; Shapiro & Teukolsky 1986), and observations of isolated pulsars ($1 < n < 2.8$; Hamil et al. 2015).

Given a rotational energy $E_{\rm rot} \propto \omega^2$, the radiated luminosity $\dot{E}_{\rm rot}$ is proportional to $\omega\dot{\omega} = \omega^{n+1}$. Hence, the time derivative of this rate, $\ddot{E}_{\rm rot}$, scales as $\omega^{2n} = \dot{E}_{\rm rot}^{2n/(n+1)}$, i.e.,

$$dt \propto \dot{E}_{\rm rot}^{-\frac{2n}{n+1}}\, d\dot{E}_{\rm rot}. \tag{1}$$

This result simply states that the amount of time $dt$ that a spinning-down NS spends radiating power in the range $\dot{E}$ to $\dot{E}_{\rm rot} + d\dot{E}_{\rm rot}$ is proportional to $\dot{E}^{-2n/(n+1)}$. It does not limit the time over which spin-down occurs. In the MDR model, the constant of proportionality scales with the square of the magnetic field strength $B$ (which can be assumed constant on long timescales), and will vary greatly between NS. This model, expanded to consider simultaneous magnetic field decay, is typically used in pulsar population synthesis (e.g., Cieślar et al. 2020). A survey measuring a population $\Phi$ of similar NS obeying Equation (1) would therefore find a distribution $d\Phi(\dot{E}_{\rm rot}) \propto \dot{E}_{\rm rot}^{-2n/(n+1)}\, d\dot{E}_{\rm rot}$. This will be the case even when the constant of proportionality between $\dot{\omega}$ and $\omega^n$—and hence $dt$ and the right-hand side of equation (1)— varies source to source, e.g., as found for pulsars by Szary et al. (2014). If NS spin-down is the underlying mechanism for powering FRBs, i.e., $\dot{E}_{\rm rot} \sim \bar{E}_{\rm FRB}$, a similar scaling in long-term repeating FRB energy $\bar{E}_{\rm FRB}$ output may be expected.

A good observable proxy for the long-term energy output of a repeating FRB $\bar{E}_{\rm FRB}$ is its repeat rate $R_0$ above some burst energy threshold $E_0$. Scaling the total energy output $\bar{E}_{\rm FRB}$, and hence $\dot{E}_{\rm rot}$, by adjusting $R_0$ implies a population $\Phi$ of repeating FRBs such that

$$d\Phi = CR_0^{\zeta}\, dR_0, \tag{2}$$

where $\zeta = -2n/(n + 1)$, i.e., $\zeta = -1.5$ for $n = 3$. The constant $C$ reflects the number of objects per Mpc$^3$. Clearly, this population will exist within a finite range of $R_0$, i.e., between a maximum rate $R_0^{\rm max}$ and minimum $R_0^{\rm min}$. A discussion of effects that may lead the observed value of $\zeta$ to deviate from these expected values is left to Section 5.

## 3. Maximum-likelihood Methods

We model the cumulative burst energy distribution of a given FRB as a power law with index $\gamma$,

$$R(E > E_0) = R_0 \left( \frac{E_0}{10^{38}\ \rm erg} \right)^{\gamma}, \tag{3}$$

giving the rate $R$ (day$^{-1}$) of bursts above an energy threshold, $E_0$. For each of 27 ASKAP-detected FRBs, James et al. (2019a) model the probability, $p(N)$, of detecting $N$ repeat bursts in follow-up observations as a function of $R_0$ and $\gamma$. The authors also investigate the effect of source spectral index $\alpha$ (fluence $F \propto \nu^{\alpha}$) and of burst times following a Weibull distribution with clustering parameter $k$. The use of a Weibull distribution does not affect the expected number of observed bursts, but rather the distribution of wait times, $\delta t$, with probability distribution

$$\frac{k}{\delta t}[\delta t\, R\, \Gamma(1 + k^{-1})]^k e^{-[\delta t\, R\, \Gamma(1+k^{-1})]^k}. \tag{4}$$

Hence $p(N)$ also depends on $k$. For brevity, from now on we write only $p(N|R_0)$, and by default use the parameter values $k = 0.34$ (Oppermann et al. 2018), $\gamma = -0.9$ (Law et al. 2017; James 2019; Lu & Piro 2019), and $\alpha = -1.5$ (Macquart et al. 2019).

The likelihood $\mathcal{L}$ of the CRAFT follow-up observations having observed two repeat bursts from FRB 171019, and none from the remaining 26 one-off bursts, is

$$\mathcal{L} = \left[ \Pi_{i=1}^{26} \int_{R_0^{\rm min}}^{R_0^{\rm max}} R_0 \Phi(R_0) p_i(N_i = 0|R_0)\, dR_0 \right]$$
$$\cdot \int_{R_0^{\rm min}}^{R_0^{\rm max}} R_0 \Phi(R_0) p_{171019}(N = 2|R_0)\, dR_0. \tag{5}$$

The first term represents the joint probability of the 26 FRBs for which $N = 0$ repeat bursts were discovered, while the second represents the probability of observing $N = 2$ repeat bursts from FRB 171019 during different observation periods with the 800 MHz receiver on the Robert C. Byrd Green Bank Telescope. Within the integrand, $R_0\Phi(R_0)$ is the a priori probability of a discovered burst originating from an FRB with rate $R_0$—the extra factor $R_0$ accounts for FRBs with greater $R_0$ producing more bursts to be discovered.

A crucial element of this analysis is to only consider the likelihood of the number of repeat bursts given the initial discovery, and discard the likelihood of observing the original burst. Since there is no way of obtaining information on repeating FRBs in a telescope's field of view from which no bursts were detected, those which are detected represent a statistically biased sample. This effect is analogous to the discovery bias associated with the detection of the Lorimer burst (Lorimer et al. 2007; Macquart & Ekers 2018), albeit applied to a single FRB, rather than an entire population.

This approach does however prevent an absolute estimate of the volumetric density of repeating FRBs, $C$, from Equation (2). Thus we choose $C$ as a normalization constant
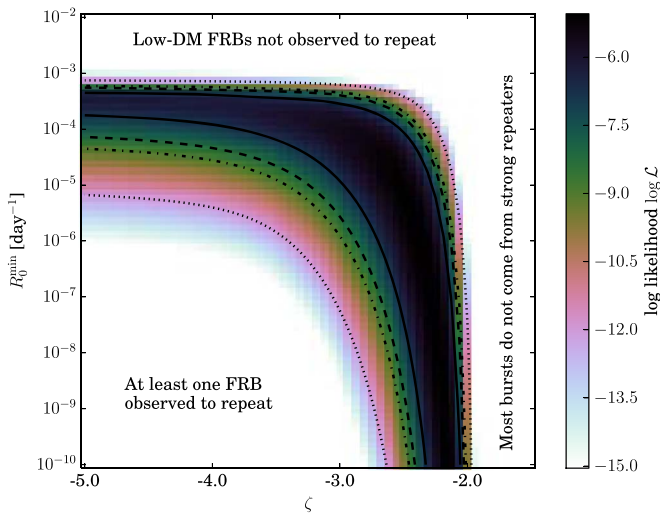
**Figure 1.** Log-likelihood $\log \mathcal{L}$ as a function of fitting parameters $R_0^{\min}$ and $\zeta$, after being marginalized over $R_0^{\max}$, for the standard parameter set $\gamma = -0.9$, $k = 0.34$, and $\alpha = -1.5$. Confidence intervals of 68%, 90%, 95%, and 99.7% are shown by solid, dashed, dotted–dashed, and dotted lines, respectively.

of the a priori probability of $R_0$:

$$C = \left( \int_{R_0^{\min}}^{R_0^{\max}} R_0 \Phi(R_0) dR_0 \right)^{-1}. \qquad (6)$$

## 4. Results

We now proceed to use the ASKAP repetition statistics to deduce limits on $\zeta$, $R_0^{\min}$, and $R_0^{\max}$. We use a brute-force calculation (evaluating $\mathcal{L}$ from Equation (5) at every point in the parameter space) rather than a minimization algorithm, and use Wilks's theorem to calculate confidence intervals (Wilks 1962). The resulting likelihood space, marginalized over $R_0^{\max}$, is shown in Figure 1.

We obtain a best-fit value of $\zeta = -2.375$. At $\zeta = -2$, the prior distribution in $R_0$ is log-uniform, while for $\zeta > -2$ it is biased toward $R_0^{\max}$. Since the CRAFT follow-up observations do not detect most ASKAP bursts as coming from strong repeaters, we constrain $\zeta \leqslant -2.13$ (90% C.L.), and exclude $\zeta \geqslant -2$ at better than 99.7% (3$\sigma$).

The observed lack of repetition from low dispersion measure (DM) bursts such as FRB 171020, which are necessarily nearby events, provides strong upper limits on their intrinsic repetition rate $R_0$. If these bursts do come from repeating objects, the minimum possible repetition rate $R_0^{\min}$ must therefore be significantly less than these limits. We obtain the constraint $R_0^{\min} < 10^{-2.9}$ day$^{-1}$ (90% C.L.). Deeper observations of low-DM FRBs, and in particular confirmation of a nearby galaxy as their host (Mahony et al. 2018), would further constrain $R_0^{\min}$.

As both $\zeta$ and $R_0^{\min}$ decrease, the prior probability mass at high $R_0$ decreases. Maintaining a finite probability of detecting FRB 171019 therefore excludes a broad region in the bottom left of Figure 1, and produces the anticorrelation in best-fit values of $\zeta$ and $R_0^{\min}$.

The resulting range of allowed values of $\zeta$, $R_0^{\min}$ is therefore an arc, or "boomerang." The region $R_0^{\min} = 10^{-3.5 \pm 0.5}$, $\zeta < -3$ represents the possibility that the two bursts observed by the Robert C. Byrd Green Bank Telescope (GBT) from

FRB 171019 were "lucky," and that its true rate is comparable to the upper limits on necessarily nearby FRBs such as 171020. In this case, the $R_0$ distribution becomes compacted around rates of $10^{-4}$–$10^{-3}$ day$^{-1}$. The region $\zeta = -2.25 \pm 0.25$, $R_0^{\min} < 10^{-5}$ represents a broad distribution of rates, with a few strongly repeating sources, and many more with much lower repetition rates. Our results alone cannot distinguish between these two scenarios.

As the preferred value of $\zeta$ is less than $-2$, the probability of high $R_0$ values is very small. Therefore, $R_0^{\max}$ can only be constrained to a lower bound of $\gtrsim 10^{-5}$ day$^{-1}$ (90% C.L.). This is clearly lower than the repetition rate of at least a few per day observed for FRB 121102 (Law et al. 2017; Oostrum et al. 2020), which thus provides a more stringent lower bound on $R_0^{\max}$. We have therefore imposed a limit of $R_0^{\max} \geqslant 4$ day$^{-1}$ for limits/results quoted in this work. Furthermore, for $R_0^{\min} = 10^{-3}$, $\zeta = -3$, bursts produced by FRBs with a rate of $R_0 = 1$ day$^{-1}$ will be a million times rare than those with rates of $10^{-3}$ day$^{-1}$. The observation of FRB 121102 therefore suggests that the allowed region $R_0^{\min} = 10^{-3.5 \pm 0.5}$, $\zeta < -3$ is implausible.

### 4.1. Analysis of Systematic Effects

The probabilities $p(N)$ from Equation (5) have been calculated for several different assumptions on the behavior of repeating FRBs. Since the primary source of information on $\Phi(R_0)$ comes from the properties of FRB 171019 compared to the 26 bursts with no observed repetition, we consider varying $p(N)$ only for FRB 171019 while holding those of the other FRBs constant. Specifically, we vary:

1. the assumptions regarding scattering and band occupancy discussed by James et al. (2019a);
2. the spectral index $\alpha$ in the range $-8 \leqslant \alpha \leqslant 0$ (Kumar et al. 2019);
3. the burst energy distribution over $-0.7 \leqslant \gamma \leqslant -1.1$ to reflect the observed range for both FRB 121102 (Law et al. 2017; Gajjar et al. 2018; James 2019) and the population as a whole (Lu & Piro 2019);
4. the Weibull clustering index over $0.29 \leqslant k \leqslant 0.4$ seen for FRB 121102 (Oppermann et al. 2018) and, for completeness, the Poisson case ($k = 1$); and
5. the redshift of FRB 171019, by taking the default value of $z = 0.39$ calculated by considering Galactic, halo, and intergalactic medium contributions only, and assuming a large excess dispersion measure such that the true redshift might be as low as $z = 0.195$.

Changing each parameter individually produces the likelihoods $\mathcal{L}$ (marginalized over $R_0^{\min}$ and $R_0^{\max}$) shown in Figure 2. The effect of varying $\gamma$ was very small, and is not shown. The remainder of the likelihoods are normalized by their maximum value, $\mathcal{L}_{\max}$.

When varying $k$ and $\gamma$, the likelihood behaves similarly to that for the standard scenario, i.e., it is maximized for $-2.5 \leqslant \zeta \leqslant -2.375$, poorly constrained at low $\zeta$ values, and strongly constrained at $\zeta \geqslant -2$.

If the spectral index is very steep ($\alpha = -8$), the discovery at 800 MHz of repeat bursts does not imply strong emission at 1.3 GHz, and constraints over the entire parameter space become very weak. The constraint $\zeta < -2$ nonetheless holds at 90% C.L. If FRB 171019 is relatively nearby ($z = 0.195$), the implied repetition rate above $10^{38}$ erg becomes lower. Given
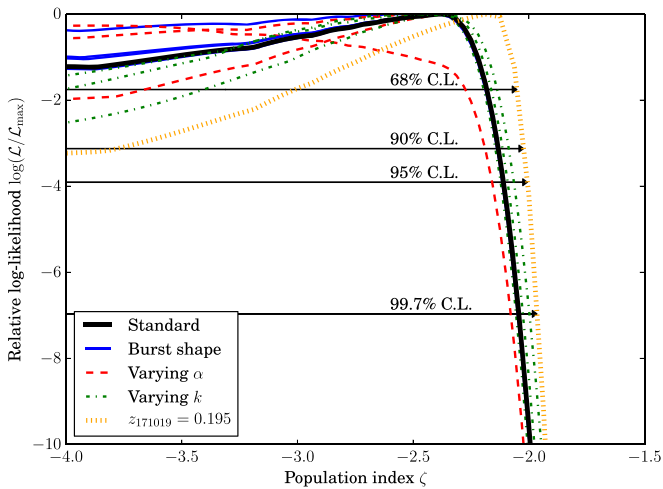
**Figure 2.** Log-likelihood $\log \mathcal{L}$ normalized by $\mathcal{L}_{\max}$, marginalized over both $R_0^{\min}$ and $R_0^{\max}$. This is shown for both the standard set of assumptions for all FRBs (thick black line), and a range of different assumptions about the properties of FRB 171019: its burst shape (blue thin solid line), spectral index $\alpha$ (red dashed line), time clustering $k$ (green dotted–dashed line), and redshift (orange dotted line), with confidence intervals as indicated.

we constrain $R_0^{\max} > 4$ day$^{-1}$, this slightly favors flatter $R_0$ distributions, with a best-fit $\zeta = -2.2$.

Expanded confidence intervals, calculated to be inclusive of all systematics, are also shown in Figure 2, and give the 90% C. L. as $\zeta \leqslant -2.02$. A similar analysis for $R_0^{\min}$ does not affect the standard limit of $R_0^{\min} < 10^{-2.9}$ day$^{-1}$ at 90% C.L.

Finally, maximum-likelihood analyses tend to provide biased parameter estimates. In the case of a power-law distribution, estimated using the procedure of Crawford et al. (1970), the bias in the estimate of the index is a factor of $(M + 1)/M$, where $M$ is the sample size. Here, for $M = 27$, this would result in a 3.8% bias. The methods used here are not identical to those of Crawford et al. (1970), however, and hence the true small-sample bias is unknown. We therefore include the possible 3.8% bias in the allowed systematic range, but do not change our nominal best-fit value of $\zeta$. Thus our 90% upper limit on $\zeta$ becomes $-1.94$.

### 4.2. Comparison with Results from CHIME

CHIME have published the detection of 18 repeating FRBs (CHIME/FRB Collaboration et al. 2019a; The CHIME/FRB Collaboration et al. 2019; Fonseca et al. 2020). The methods outlined here cannot be applied to this sample, however, since nondetections of repetition for equivalent observation periods have not been published. An approximate treatment can be found in the methods of James et al. (2019b), by observing that a threshold of $N_{\mathrm{th}} = 2$ detected bursts is required to publish a repeating FRB. Thus the statistic $s = N_{\mathrm{rep}}/N_{\mathrm{th}}$, where $N_{\mathrm{rep}}$ is the number of repeat bursts, should follow the same power-law distribution as $R_0$. Applying this treatment exactly would require that the observed burst number $N_{\mathrm{rep}}$ is equal to its expectation value, that the maximum rate $R_0^{\max}$ is much larger than the observed rates, that $N_{\mathrm{rep}}$ be allowed to take continuous values, and that no further bursts from FRB 180814.J0422+73 beyond those reported by CHIME/FRB Collaboration et al. (2019a) had been detected by the time of publication of the latter 17 repeaters (thus, we do not include the extra bursts from FRB 180916.J0158+65 published by The CHIME/FRB Collaboration et al. 2020). With these admittedly strong caveats,

this method yields a bias-corrected value of $\zeta = -2.7^{+0.9}_{-1.1}$ (90% C.L.) for the CHIME sample. This is clearly consistent with the results presented here, and places a useful lower limit on $\zeta$ of $-3.8$, albeit a not very robust one.

### 5. Discussion—Limiting FRB Progenitor Models

We have adopted a power-law form for the rate distribution of repeating FRBs using a model whereby mean FRB energy $\bar{E}_{\mathrm{FRB}}$ is proportional to the spin-down power of NS $\dot{E}_{\mathrm{rot}}$. However, a range of different FRB progenitor models also predict a power-law distribution. Here, we show how our measured value of the power-law index $\zeta = -2.375$ ($\zeta < -1.94$ at 90% C.L.) can be used to constrain these models. In particular, we also consider magnetar and binary scenarios, which The CHIME/FRB Collaboration et al. (2020) discuss as possible explanations for their recent observation of a $16.35 \pm 0.18$ day periodicity in FRB 180916.J0158+65.

1. NS spin-down: linear proportionality. In the case of FRBs with energy linearly proportional to NS spin-down discussed in Section 2, $\zeta$ can be related to the braking index $n$ via $\zeta = -2n(n + 1)^{-1}$, i.e., $n = -\zeta(2 + \zeta)^{-1}$. Our measurements correspond to $n = -6.3$, with allowed values $n < -1$, $n > 32$ at 90% C.L. This excludes the expected value of $n = 3$ ($\zeta = -1.5$) expected for MDR. It also excludes models based on the observed braking indices of isolated neutron stars, which tend to exhibit $n < 3$ (Hamil et al. 2015).

2. NS spin-down: nonlinear proportionality. Since the mechanism of FRB emission is not known, the mean FRB energy $\bar{E}_{\mathrm{FRB}}$ may scale nonlinearly with NS spin-down power. For instance, Faucher-Giguère & Kaspi (2006) use pulsar population synthesis to conclude that pulsar luminosity $L \propto \dot{E}_{\mathrm{rot}}^{0.5}$. A more-general model where $\bar{E}_{\mathrm{FRB}} \propto \dot{E}_{\mathrm{rot}}^{\ell}$, when inserted into Equation (2), produces $\zeta = [-2n/(n + 1) + 1]/\ell - 1$. In the case of $n = 3$, we constrain $\ell < 0.0.53$ at 90% C.L, i.e., the value of $\ell = 0.5$ derived from known pulsars by Faucher-Giguère & Kaspi (2006) is consistent with our results, as is the lack of dependence ($\ell \sim 0$) found by Szary et al. (2014).

3. NS spin-down: variable birth rate. If FRBs are born (or first become visible, in the case of their being placed inside an obscuring nebula, as may be the case for FRB 121102; Metzger et al. 2017) with an initial FRB emission rate $R_b$, then the observed population repeating at rate $R_0$ will be proportional to the probability of a birth rate above $R_0$, $p(R_b > R_0)$. For example, if $p(R_b > R_0) \propto R_b^{\beta}$ ($\beta < 0$), then $\zeta = -2n/(n + 1) + \beta$. In the case of $n = 3$, this constrains $\beta < -0.44$ at 90% C.L.

4. Magnetar field decay: ambipolar diffusion over a constant length scale. The model of a young magnetar embedded within a nebula proposed for FRB 121102 by Metzger et al. (2017) is modeled by Margalit & Metzger (2018) as having a magnetic dissipation timescale $t_{\mathrm{mag}}$ ($\equiv B dt/dB$) of $400 L_{\mathrm{km}}^{1.6} B_{16}^{-1.2}$ yr. This is based on the calculation by Beloborodov & Li (2016) of magnetar heating through ambipolar diffusion, and assumes that fluctuations $\delta B$ in the magnetic field strength $B_{16}$ (units of $10^{16}$ G) are proportional to $B$ over a length scale $L_{\mathrm{km}}$ (in km). If $L_{\mathrm{km}}$ remains constant, then this implies $dt \propto B^{-2.2} dB$. If such

an object emits FRBs with energy $\bar{E}_{\mathrm{FRB}} \propto B$, this implies $\zeta = -2.2$, which is consistent with our constraints on $\zeta$.

5. Magnetar field decay: ambipolar diffusion over a variable length scale. Ambipolar diffusion acts to smooth magnetic field fluctuations $\delta B$ over all length scales $L_{\mathrm{km}}$. As Beloborodov & Li (2016) discuss, if initially $(\delta B)^2 \propto L_{\mathrm{km}}^{-\alpha_B}$ for some index $\alpha_B$, then $L_{\mathrm{km}}$ will gradually increase over the magnetar lifetime. In this model, $dt \propto B^{-2.2+3.2/\alpha_B}$, and hence if $\bar{E}_{\mathrm{FRB}} \propto B$, we reject the range $\alpha_B < 12.3$ at 90% C.L.

6. Magnetic field interactions of compact binaries. FRB emission has been proposed to originate from the magnetic field interactions of compact binaries, e.g., an NS–NS system. Wang et al. (2018) consider several scenarios, each predicting energy output of the form $\bar{E}_{\mathrm{FRB}} \sim \dot{E} \propto a^x$, where $a$ is the semimajor axis of the orbit, and $-7 \leqslant x \leqslant -2$, depending on the scenario considered. Given gravitational-wave (GW) orbital decay $da/dt \propto a^{-3}$, this produces $dt \propto \dot{E}^\zeta d\dot{E}$ where $\zeta = 4x^{-1} - 1$. We thus obtain $x \geqslant -4.2$ at 90% C.L. This excludes the unipolar inductor and magnetic reconnection scenarios for NS–BH and NS–NS binaries in the case where the companion star has a low surface magnetic field, which predict $x = -7$ (Wang et al. 2018).

Our measurement of $\zeta$ can thus be used to constrain the emission mechanism of FRBs for several scenarios. In doing so, we have considered various relationships between the mean radiated FRB power $\bar{E}_{\mathrm{FRB}}$—here proxied by $R_0$—and the energy loss of the system $\dot{E}$. However, the exact relationship will be determined by the "microphysics" of FRB emission, of which there are many models, and we consider only a fraction (see, e.g., Platts et al. 2019 for a review). We encourage further development of expectations for the long-term luminosity evolution in FRB progenitor scenarios to allow a detailed comparison to measured values of the burst rate index $\zeta$.

It may also be that mean FRB power $\bar{E}_{\mathrm{FRB}}$ is only weakly related to the energy loss of the progenitor. Again using the analogy with Galactic pulsars, Szary et al. (2014) find almost no relationship between radio luminosity $L$ and spin-down power $\dot{E}_{\mathrm{rot}}$, with $L$ being fixed for the lifetime of the system. Applied to FRBs, the repetition rate $R_0$ would then carry no information regarding $\dot{E}_{\mathrm{rot}}$, but our measured value of $\zeta$ would then reflect whatever physics determines the initial distribution of $R_0$.

A further consideration is cosmological source evolution. If the time period over which an FRB is active is comparable to cosmological timescales, the $R_0$ distribution in the current epoch could be dominated by (for example) low-$R_0$ objects formed near the peak of star-forming activity, while measurements of $R_0$ from FRB observations, which probe to at least $z = 1$ (Shannon et al. 2018), may be dominated by high-$R_0$ objects born at previous epochs. Since our model for $R_0$ does not specify the spin-down time—and these effects act to counter each other—we leave the investigation of them to a future work.

In light of these considerations, we note that any distribution —not just a power law—can be fitted to measurements of, and limits on, the repetition rate $R_0$, using the methods outlined here. To allow such fitting requires the exposure times, sensitivities, and the number of observed bursts, for all FRBs in a sample over the same time period.

Observationally, the publication of all one-off and repeating FRBs observed by the CHIME Collaboration for the same time period would allow better constraints to be derived from this experiment. The detection of a repeating FRB with an intrinsically low rate would also place better constraints on the repeating population. This may be best accomplished through the follow-up of low-DM, i.e., nearby, FRBs, the more-frequent low-energy emission of which could be detectable even if their rate of emission above $10^{38}$ erg is very low. The recent localization of (The CHIME/FRB Collaboration et al. 2019) repeating FRB 180916.J0158+65 to a nearby galaxy at $z = 0.0337 \pm 0.0002$ (Marcote et al. 2020) allows its absolute rate to be calculated. However, it is relatively high: four bursts above $5 \times 10^{36}$ erg (assuming a 1 GHz bandwidth) in a 5.5 hr period were observed, corresponding to $R_0 = 1.2$ day$^{-1}$ (above $10^{38}$ erg) assuming $\gamma = -0.9$. Thus it does not further constrain the values of $R_0^{\mathrm{min}}$ and $R_0^{\mathrm{max}}$ found here.

## 6. Conclusion

Using the results of FRB follow-up observations by the CRAFT Collaboration, we have analyzed the scenario that all FRBs originate from a single source population. This necessarily requires repeating objects with a broad distribution of the intrinsic repetition rate $R_0$ of bursts with energies greater than $10^{38}$ erg. We find that the repeating FRB population is consistent with a power-law distribution $p(R_0) \sim R_0^\zeta$ of burst rates, with index $\zeta < -2.13$ (90% C.L.). The distribution must extend below $R_0^{\mathrm{min}} < 10^{-2.9}$ day$^{-1}$. Including a range of systematic effects produces a 90% C.L. upper bound $\zeta < -1.94$. This result is also consistent with the available statistics on the CHIME sample of repeating FRBs ($\zeta = -2.7^{+0.9}_{-1.1}$ at 90% C.L.). Values of $\zeta \lesssim -3$ are unlikely due to the existence of high-rate repeaters such as FRB 121102, so we expect the true value to lie in the range $-3 \leqslant \zeta \leqslant -1.94$.

We have demonstrated how this result can be used to limit different progenitor models of repeating FRBs. It excludes FRBs with burst rate proportional to neutron star spin-down power with braking indices $n < 32$, i.e., MDR ($n = 3$), and the braking indices observed for known pulsars ($n \lesssim 3$). It is consistent, however, with FRB rates scaling with the square root of spin-down power, with magnetic field decay due to ambipolar diffusion over a constant length scale, and with some, but not all, models of FRBs from magnetic field interactions in compact binaries decaying due to GW radiation.

## ORCID iDs

C. W. James ● https://orcid.org/0000-0002-6437-6176
S. Osłowski ● https://orcid.org/0000-0003-0289-0732
C. Flynn ● https://orcid.org/0000-0002-4796-745X
P. Kumar ● https://orcid.org/0000-0003-1913-3092
K. Bannister ● https://orcid.org/0000-0003-2149-0363
S. Bhandari ● https://orcid.org/0000-0003-3460-506X
W. Farah ● https://orcid.org/0000-0002-0161-7243
M. Kerr ● https://orcid.org/0000-0002-0893-4073
D. R. Lorimer ● https://orcid.org/0000-0003-1301-966X
J.-P. Macquart ● https://orcid.org/0000-0001-6763-8234
C. Ng ● https://orcid.org/0000-0002-3616-5160
D. C. Price ● https://orcid.org/0000-0003-2783-1608
H. Qiu ● https://orcid.org/0000-0002-9586-7904
R. Spiewak ● https://orcid.org/0000-0002-6730-3298

## References

Bannister, K. W., Deller, A. T., Phillips, C., et al. 2019, Sci, 365, 565
Beloborodov, A. M., & Li, X. 2016, ApJ, 833, 261
Caleb, M., Spitler, L. G., & Stappers, B. W. 2018, NatAs, 2, 839
CHIME/FRB Collaboration, Amiri, M., Bandura, K., et al. 2019a, Natur, 566, 235
CHIME/FRB Collaboration, Amiri, M., Bandura, K., et al. 2019b, Natur, 566, 230
Cieślar, M., Bulik, T., & Osłowski, S. 2020, MNRAS, 492, 4043
Crawford, D. F., Jauncey, D. L., & Murdoch, H. S. 1970, ApJ, 162, 405
Farah, W., Flynn, C., Bailes, M., et al. 2018, MNRAS, 478, 1209
Faucher-Giguère, C.-A., & Kaspi, V. M. 2006, ApJ, 643, 332
Fedorova, V. A., & Rodin, A. E. 2019, ATel, 12899, 1
Fonseca, E., Andersen, B. C., Bhardwaj, M., et al. 2020, ApJL, 891, L6
Gajjar, V., Siemion, A. P. V., Price, D. C., et al. 2018, ApJ, 863, 2
Hamil, O., Stone, J. R., Urbanec, M., & Urbancová, G. 2015, PhRvD, 91, 063007
Hessels, J. W. T., Spitler, L. G., Seymour, A. D., et al. 2019, ApJL, 876, L23

Hunter, J. D. 2007, CSE, 9, 90
James, C., Osłowski, S., CFlynn, C., et al. 2019a, MNRAS, in press (arXiv:1912.07847)
James, C. W. 2019, MNRAS, 486, 5934
James, C. W., Ekers, R. D., Macquart, J.-P., Bannister, K. W., & Shannon, R. M. 2019b, MNRAS, 483, 1342
Kashiyama, K., Ioka, K., & Mészáros, P. 2013, ApJL, 776, L39
Kumar, P., Shannon, R. M., Osłowski, S., et al. 2019, ApJL, 887, L30
Law, C. J., Abruzzo, M. W., Bassa, C. G., et al. 2017, ApJ, 850, 76
Lorimer, D. R., Bailes, M., McLaughlin, M. A., Narkevic, D. J., & Crawford, F. 2007, Sci, 318, 777
Lu, W., & Piro, A. L. 2019, ApJ, 883, 40
Lyubarsky, Y. 2014, MNRAS, 442, L9
Macquart, J.-P., Bailes, M., Bhat, N. D. R., et al. 2010, PASA, 27, 272
Macquart, J.-P., & Ekers, R. D. 2018, MNRAS, 474, 1900
Macquart, J. P., Shannon, R. M., Bannister, K. W., et al. 2019, ApJL, 872, L19
Mahony, E. K., Ekers, R. D., Macquart, J.-P., et al. 2018, ApJL, 867, L10
Marcote, B., Nimmo, K., Hessels, J. W. T., et al. 2020, Natur, 577, 190
Margalit, B., & Metzger, B. D. 2018, ApJL, 868, L4
Metzger, B. D., Berger, E., & Margalit, B. 2017, ApJ, 841, 14
Oostrum, L. C., Maan, Y., van Leeuwen, J., et al. 2020, A&A, 635, A61
Oppermann, N., Yu, H.-R., & Pen, U.-L. 2018, MNRAS, 475, 5109
Oslowski, S., Shannon, R. M., Jameson, A., et al. 2018, ATel, 11385, 1
Patek, C. & CHIME/FRB Collaboration 2019, ATel, 13013, 1
Pen, U.-L., & Connor, L. 2015, ApJ, 807, 179
Platts, E., Weltman, A., Walters, A., et al. 2019, PhR, 821, 1
Prochaska, J. X., Macquart, J.-P., McQuinn, M., et al. 2019, Sci, 366, 231
Ravi, V. 2019, NatAs, 3, 928
Ravi, V., Shannon, R. M., Bailes, M., et al. 2016, Sci, 354, 1249
Shannon, R. M., Macquart, J.-P., Bannister, K. W., et al. 2018, Natur, 562, 386
Shapiro, S. L., & Teukolsky, S. A. 1986, Black Holes, White Dwarfs and Neutron Stars: The Physics of Compact Objects (New York: Wiley)
Spitler, L. G., Cordes, J. M., Hessels, J. W. T., et al. 2014, ApJ, 790, 101
Spitler, L. G., Scholz, P., Hessels, J. W. T., et al. 2016, Natur, 531, 202
Szary, A., Zhang, B., Melikidze, G. I., Gil, J., & Xu, R.-X. 2014, ApJ, 784, 59
Totani, T. 2013, PASJ, 65, L12
The CHIME/FRB Collaboration, Amiri, M., Andersen, B. C., et al. 2020, arXiv:2001.10275
The CHIME/FRB Collaboration, Andersen, B. C., Bandura, K., et al. 2019, ApJL, 885, L24
van der Walt, S., Colbert, S. C., & Varoquaux, G. 2011, CSE, 13, 22
Virtanen, P., Gommers, R., Oliphant, T., et al. 2019, arXiv:1907.10121
Wang, J.-S., Peng, F.-K., Wu, K., & Dai, Z.-G. 2018, ApJ, 868, 19
Wang, J.-S., Yang, Y.-P., Wu, X.-F., Dai, Z.-G., & Wang, F.-Y. 2016, ApJL, 822, L7
Wilks, S. 1962, Mathematical Statistics (New York: Wiley)
Zhang, B. 2014, ApJL, 780, L21
Zhang, B.-B., & Zhang, B. 2017, ApJL, 843, L13